



Comparative Molecular Field Analysis of Colchicine Inhibition and Tubulin Polymerization for Combretastatins Binding to the Colchicine Binding Site on β -Tubulin

Milton L. Brown, Jayson M. Rieger and Timothy L. Macdonald*

Chemistry Department, University of Virginia, McCormick Road, PO Box 400319, Charlottesville, VA 22904-4319, USA

Received 10 December 1999; accepted 18 February 2000

Abstract—A molecular modeling study using Comparative Molecular Field Analysis (CoMFA) was undertaken to develop a predictive model for combretastatin binding to the colchicine binding site of tubulin. Furthermore, we examined the potential contribution of lipophilicity ($\log P$) and molecular dipole moment and were unable to correlate these properties to the observed biological data. In this study we first confirmed that tubulin polymerization inhibition (IC_{50}) correlated ($R^2=0.92$) with [3H]colchicine displacement. Although these data correlated quite well, we developed two independent models for each set of data to quantify structural features that may contribute to each biological property independently. To develop our predictive model we first examined a series of molecular alignments for the training set and ultimately found that overlaying the respective trimethoxyphenyl rings (A ring) of the analogues generated the best correlated model. The CoMFA yielded a cross-validated $R^2=0.41$ (optimum number of components equal to 5) for the tubulin polymerization model and an $R^2=0.38$ (optimum number of components equal to 5) for [3H]colchicine inhibition. Final non-cross-validation generated models for tubulin polymerization (R^2 of 0.93) and colchicine inhibition (R^2 of 0.91). These models were validated by predicting both biological properties for compounds not used in the training set. These models accurately predicted the IC_{50} for tubulin polymerization with an R^2 of 0.88 ($n=6$) and those of [3H]colchicine displacement with an R^2 of 0.80 ($n=7$). This study represents the first predictive model for the colchicine binding site over a wide range of combretastatin analogues. © 2000 Elsevier Science Ltd. All rights reserved.

Introduction

Microtubules are essential components of cell structure and are involved in many important cellular processes including mitosis, morphogenesis, intracellular transport and secretion.¹ Tubulin, the basic subunit of microtubules, is composed of an α,β -heterodimer and the polymerization of this heterodimer complex leads to microtubule formation. The binding of small molecules and other proteins, termed microtubule associated proteins (MAPs), to tubulin can result in the stabilization or destabilization of microtubule formation. Combretastatins, derived from the South African tree *Combretum caffrum*, have been identified as competitive inhibitors of the colchicine binding site on β -tubulin—one of several distinct binding regions on this protein defined by its affinity for colchicine (**1**).² Compounds such as the taxoids and vinca alkaloids, which interact with the other domains on tubulin, have also been synthesized and evaluated.

The relatively simple structure and high affinity of combretastatins for the colchicine binding site has led to the synthesis and subsequent evaluation of a large number of combretastatin analogues.^{3–6} Combretastatin A-4 (**2**) has been entered into clinical trials, but unfortunately these trials have been met with limited success due to the drug's poor solubility.⁷ Consequently, a more soluble phosphate prodrug of combretastatin A-4 is currently undergoing evaluation. Thus, novel compounds derived from the combretastatin core continue to hold interest as potential therapeutic targets.

Temperature-dependent specific binding of colchicine to a high affinity site on β -tubulin results in a change in the secondary structure of β -tubulin and the α,β -dimer. As a consequence of this change in secondary structure, dimer assembly is inhibited and a partial unfolding of the protein occurs.⁶ It is believed that, in this manner, colchicine as well as combretastatins disrupt tubulin stability and ultimately promote cell death.

We have previously been interested in elucidating both the interaction of colchicine^{8–10} and its analogues with

*Corresponding author. Tel.: +1-804-924-7718; fax: +1-804-982-2302; e-mail: tlm@virginia.edu

tubulin as well as structure–activity relationships (SAR) that result in potent binding of compounds to the β -tubulin colchicine binding site. Previous SAR work on combretastatins indicates that a *cis* ethylene linkage between the two aryl rings leads to the greatest activity.¹¹ Further studies⁵ have shown the importance of the 5 methoxy and 3' hydroxy groups (see Fig. 1).

Several models have been proposed for predicting the activity of combretastatin binding to the colchicine binding site, but these models have met with limited success and utility. A study of dihydrocombretastatin and combretastatin A-2 derivatives generated good correlation with tubulin polymerization ($R^2=0.98$). Unfortunately this model was unable to predict ($R^2=0.17$) inhibition of tubulin polymerization for combretastatin A-4.¹² Another model has attempted to correlate structural features with leukemic cell line cytotoxicity, but was limited by the number of structural variations included and an inability to accurately predict the experimental data of the test set.¹¹ Both of these were 2-dimensional (2-D) models and neither included the native ligand, colchicine, or were predictive across multiple combretastatin subclasses.

Comparative molecular field analysis (CoMFA) has been a useful technique in defining important 3-dimensional (3-D) properties associated with the optimum binding of ligands to a binding site. CoMFA samples the differences in steric and electrostatic fields surrounding a set of compounds and maps these differences to biological activity. Successful CoMFA models have already been developed for the tubulin binding regions of paclitaxel¹³ and podophyllotoxin,¹⁴ although none are presently available for the colchicine site.

With this in mind, we examined combretastatin SAR through CoMFA in an effort to construct a global predictive combretastatin model for the inhibition of tubulin polymerization and colchicine binding. In this study, we correlated $\log P$ and molecular dipole moment with inhibition of tubulin polymerization and colchicine binding for combretastatin analogues **2–22**; employed CoMFA to correlate the inhibition of [³H]colchicine binding and tubulin polymerization to steric and electrostatic differences of combretastatin analogues **2–22**; developed a predictive model and tested the model by predicting the inhibition of tubulin polymerization and colchicine binding for colchicine, combretastatins, phenstatin and podophyllotoxin.

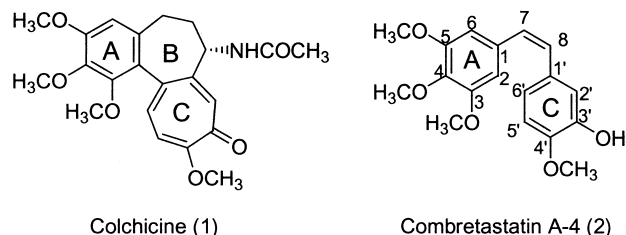


Figure 1. Structure of colchicine and combretastatin A-4, two compounds with high affinity for the colchicine binding site.

Results and Discussion

There is tremendous literature precedence for combretastatin analogues inhibiting tubulin polymerization with an assumed action through the colchicine binding site. Because our goal was to construct a CoMFA of the colchicine binding site, we decided to confirm that a correlation existed for our training set. This necessitated that we include only analogues in our training set that inhibited tubulin polymerization through action at the colchicine site. Therefore, only literature compounds where both tubulin polymerization and [³H]colchicine inhibition were available were included in our model. Our first pass attempt to correlate tubulin polymerization and [³H]colchicine inhibition obtained from multiple studies provided a non-optimal $R^2=0.83$. This prompted us to normalize all the data to an internal standard of combretastatin A-4 (**2**). Upon normalization, we obtained an improved correlation of $R^2=0.92$, as seen in Figure 2 for our combretastatin training set (Table 1).

In general, the best inhibitors of the tubulin polymerization and colchicine binding were unsaturated combretastatins. However, the clustering of compounds from both saturated and unsaturated structural types of combretastatins in Figure 2 (i.e., **6, 9, 10, 12, 13, 19, 20** and **22**) suggest that there are other structural and/or electronic properties important for both inhibition of tubulin polymerization and the [³H]colchicine binding. The only significant outlier, compound **5**, inhibits [³H]colchicine binding by 14%. This suggests that compounds like **5** which bind in this poor range (less than 20%) may inhibit the polymerization of tubulin by a different interaction or represent inaccurate biological data. Further, these results emphasize the importance of reporting both types of experimental data.

Two other reported potential properties for combretastatin binding to β -tubulin include $\log P$ and dipole, as

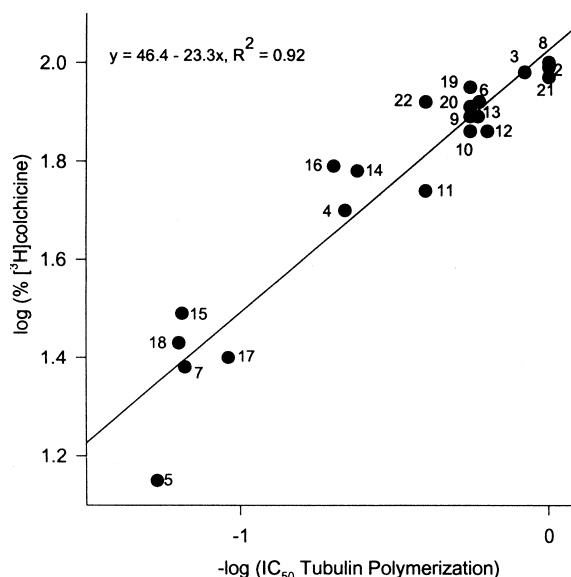
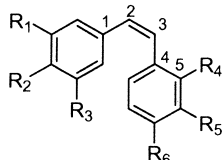
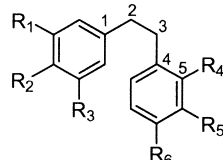
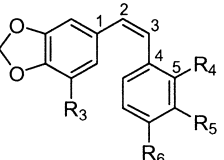
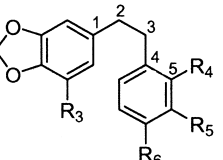
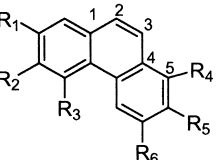


Figure 2. Plot of $-\log(\text{IC}_{50} \text{ tubulin polymerization})$ versus $\log(\% [\text{^3H}] \text{colchicine inhibition})$ for the training set.

Table 1. Tubulin polymerization and [³H]colchicine inhibition values for the training set

														
2-12			13-19			20-21			22			23		
Compound	R ₁	R ₂	R ₃	R ₄	R ₅	R ₆	Inhibition of tubulin polymerization	Normalized tubulin polymerization	% [³ H]colchicine inhibition					
2	OCH ₃	OCH ₃	OCH ₃	H	OH	OCH ₃	1.2 ^a	1	97 ^a					
3	OCH ₃	OCH ₃	OCH ₃	H	H	OCH ₃	2.2 ^b	1.2	95 ^b					
4	OCH ₃	OCH ₃	OCH ₃	H	OCH ₃	H	8.8 ^b	4.6	50 ^b					
5	OCH ₃	OCH ₃	OCH ₃	H	H	H	36 ^b	18.9	14 ^b					
6	OCH ₃	OCH ₃	OCH ₃	H	H	N(Me) ₂	3.4 ^b	1.8	83 ^b					
7	OCH ₃	OCH ₃	OCH ₃	H	H	OAc	29 ^b	15.3	24 ^b					
8	OCH ₃	OCH ₃	OCH ₃	OH	OH	OCH ₃	12.5 ^c	1	99 ^c					
9	OH	OCH ₃	OCH ₃	H	OH	OCH ₃	4.5 ^c	1.8	78 ^c					
10	OCH ₃	OCH ₃	OCH ₃	Cl	H	OCH ₃	3.5 ^b	1.8	73 ^b					
11	OCH ₃	OCH ₃	OCH ₃	H	H	Cl	4.8 ^b	2.5	55 ^b					
12	OCH ₃	OCH ₃	OCH ₃	H	H	Br	3.1 ^b	1.63	73 ^b					
13	OCH ₃	OCH ₃	OCH ₃	H	OH	OCH ₃	3.3 ^b	1.73	79 ^b					
14	OCH ₃	OCH ₃	OCH ₃	H	H	OCH ₃	7.9 ^b	4.2	65 ^b					
15	OCH ₃	OCH ₃	OCH ₃	H	H	N(Me) ₂	29 ^b	15.3	31 ^b					
16	OCH ₃	H	OCH ₃	H	OH	OCH ₃	12.5 ^c	5	62 ^c					
17	OCH ₃	H	OCH ₃	H	OH	OH	27.5 ^c	11	25 ^c					
18	OH	OCH ₃	OCH ₃	H	OH	OCH ₃	40 ^c	16	27 ^c					
19	OCH ₃	OCH ₃	OCH ₃	OH	OH	OCH ₃	4.5 ^c	1.8	82 ^c					
20	NA	NA	OCH ₃	H	OH	OCH ₃	4.5 ^c	1.8	90 ^c					
21	NA	NA	OCH ₃	OH	OH	OCH ₃	2.5 ^c	1	94 ^c					
22	NA	NA	OCH ₃	OH	OH	OCH ₃	6.3 ^c	2.5	84 ^c					
23	OCH ₃	OCH ₃	OCH ₃	H	OH	OCH ₃	100 ^c	40 ^c	ND ^d					

^aData from ref 4.^bReported in ref 25.^cReported in ref 6.^dNo data.

reported in Table 2. Log *P* has previously been correlated for compounds that bind to β-tubulin. Specifically, anti-tumor potency and log *P* for colchicine and colchicine analogues demonstrated a parabolic dependence.^{15,16} Nandy et al. also suggested that lipophilicity correlated well with the Hansch–Fujita π constant for substitutions on the B-ring (in our nomenclature the C-ring).¹¹ Because of these precedents, we sought to examine this property as a potential predictive component. In this report we were unable to obtain a correlation for log *P* and tubulin polymerization using either linear regressions or polynomial (0–3rd order) regressions. Consistent with this observation, an equally poor statistical relationship ($R^2 < 0.13$) was also obtained between log *P* and [³H]colchicine binding for the training set.

The importance of group dipole effects between combretastatins and β-tubulin has also been described.²⁴ In this study, we have found a lack of correlation between tubulin polymerization and [³H]colchicine with dipole ($R^2 = 0.01$, $R^2 = 0.02$, respectively). While individual C-ring dipoles may be important, the net dipole for the entire molecule does not provide for a useful property in predicting biological activity.

The molecular alignment of compounds in CoMFA is probably one of the most important aspects of designing a successful model. We explored several possible alignments to obtain a valid model. Ultimately, we achieved success by fitting all six of the phenyl ring carbons of the A-ring and placing the trimethoxy groups in the conformation of the X-ray structure of colchicine.²¹ This fit generated the best correlation for the diverse training set of combretastatins. These data are summarized in Tables 3–6 and Figures 3–6. Evaluation of the independently derived CoMFA models for inhibition of tubulin polymerization ($R^2 = 0.93$) and [³H]colchicine ($R^2 = 0.91$) revealed similar percent steric and electrostatic components (see Tables 5 and 6). However, graphical examinations of the CoMFA fields as seen in Figures 7 and 8 reveal a different distribution of these components. This observation is insightful and may suggest differences in steric and electronic requirements for tubulin inhibition and colchicine. Support for this is further demonstrated by each model correlating different conformations for the test set in Table 9. For example, tubulin polymerization CoMFA best predicted lowest energy conformations for compounds **24b**, **27c** and **28b** as compared with the [³H]colchicine CoMFA which accurately predicted **24a**, **27a** and **28a**. This further emphasizes the need for

Table 2. Physicochemical and conformational data for compounds in training set

Compound	Energy (kcal/mol)	Torsion angle C1, C2, C3, C4	Torsion angle C2, C3, C4, C5	Dipole ^a	Log <i>P</i>
2	13.1	−3.8	137.5	2.35	3.81
3	12.9	−3.8	NA	2.30	3.14
4a	12.8	−3.9	137.8	3.57	3.10
4b	10.9	−4.3	−45.1	1.46	
5	11.2	−3.9	NA	2.52	3.08
6	9.9	−3.9	NA	2.66	4.64
7a	13.6	−3.8	NA	1.83	2.50
7b	13.1	−3.9	NA	3.60	
8	14.9	−3.5	135	3.32	3.14
9a	11.5	−3.7	−42.1	2.00	3.16
9b	13.0	−3.7	137.1	2.68	
10a	11.8	−3.6	135	1.26	3.81
10b	1.26	−3.2	−51.2	1.77	
11	10.6	−3.8	NA	2.80	3.79
12	10.5	−3.8	NA	2.45	3.94
13	6.0	55.8	88.6	1.42	4.35
14	5.8	55.0	NA	1.80	5.02
15	3.4	56.7	NA	2.85	5.18
16a	4.9	56.0	87.0	1.37	4.37
16b	4.9	53.3	−94.8	2.34	
17a	4.4	54.6	85.4	1.80	3.74
17b	4.3	54.9	−92.7	2.69	
18a	4.4	55.6	87.4	0.83	3.70
18b	4.0	46.0	−92.9	2.52	
19a	6.2	54.7	85.8	2.64	3.68
19b	5.2	46.6	−92.6	2.60	
20a	23.4	−3.6	137.6	0.20	2.63
20b	24.8	−3.6	−40.9	1.31	
21a	25.7	−3.3	−42.7	1.87	1.96
21b	25.3	−3.5	135.0	1.22	
22a	16.5	56.4	84.7	0.60	3.17
22b	16.0	54.2	−90.9	2.52	
23	13.7	5.7	179.0	4.25	

^aDipole calculated using the AM1 MOPAC interface with SYBYL.

both types of data in evaluating and designing new analogues.

To test the validity of our models we predicted compounds that were not in our original training set. These data are summarized in Tables 7–9. The accuracy of our predictions ($R^2=0.88$ for tubulin polymerization and $R^2=0.80$ for [³H]colchicine in Figures 9 and 10) demonstrates the validity and utility of both of our models in describing interactions of combretastatin with β -tubulin. However, this simple fit was not sufficient to explain the binding of other classes of ligands such as **1**, **31** and **32** to the colchicine binding site. The poor prediction of these molecules using this first generation combretastatin model with the simple phenyl ring fit is highly suggestive of a different pharmacophore¹⁷ that can explain the binding of all classes of compounds reported to potentially inhibit tubulin polymerization and competitively displace [³H]colchicine. Studies are currently under way in our laboratory to extract a pharmacophore and develop a fit that is inclusive of multiple reported structural classes that bind to the colchicine binding site.

Table 3. Preliminary and final non-cross-validated CoMFA values for tubulin polymerization

Compound	Preliminary non-cross-validated model (log 1/IC ₅₀)			Final non-cross-validated model (log 1/IC ₅₀)		
	obs	pred	res	obs	pred	res
2	0.00	−0.05	0.05	0.00	−0.03	0.03
3	−0.08	−0.09	0.01	−0.08	−0.11	0.03
4a	−0.66	−0.61	−0.05	−0.66	−0.61	−0.05
4b	−0.66	−0.78	0.12			
5	−1.28	−0.86	−0.42	−1.28	−0.96	−0.32
6	−0.26	−0.60	0.35	−0.26	−0.42	0.17
7a	−1.18	−1.13	−0.05	−1.18	−1.16	−0.03
7b	−1.18	−1.30	0.12			
8	0.00	0.08	−0.08	0.00	−0.01	0.01
9a	−0.26	−0.45	0.19			
9b	−0.26	−0.13	−0.13	−0.26	−0.31	0.05
10a	−0.26	−0.01	−0.24			
10b	−0.26	−0.15	−0.11	−0.26	−0.10	−0.16
11	−0.40	−0.50	0.10	−0.40	−0.45	0.05
12	−0.20	−0.55	0.35	−0.20	−0.47	0.27
13	−0.23	−0.48	0.25	−0.23	−0.41	0.18
14	−0.62	−0.43	−0.19	−0.62	−0.56	−0.07
15	−1.18	−1.07	−0.11	−1.18	−1.18	0.01
16a	−0.70	−0.67	−0.03	−0.70	−0.57	−0.13
16b	−0.70	−0.56	−0.14			
17a	−1.04	−1.02	−0.02	−1.04	−1.10	0.06
17b	−1.04	−0.97	−0.07			
18a	−1.20	−1.00	−0.20			
18b	−1.20	−1.14	−0.07	−1.20	−1.33	0.12
19a	−0.26	−0.24	−0.02	−0.26	−0.29	0.04
19b	−0.26	−0.43	0.17			
20a	−0.26	−0.14	−0.11			
20b	−0.26	−0.27	0.02	−0.26	−0.10	−0.16
21a	0.00	−0.01	0.01	0.00	0.07	−0.07
21b	0.00	−0.01	0.01			
22a	−0.40	−0.47	0.07	−0.40	−0.41	0.02
22b	−0.40	−0.62	0.22			
23	−1.60	−1.53	−0.07	−1.60	−1.57	−0.03

Conclusion

We developed a CoMFA that results in models that rationalized both tubulin polymerization and [³H]colchicine binding. This study has produced the first predictive models for multiple structural types of combretastatins, including an accurate prediction of combretastatin A-4. We are currently pursuing the development of a model that is more global and capable of predicting the biological properties of compounds from several different structural classes, such as colchicines and podophyllotoxins.

Experimental

Normalization of biological data

All data were normalized to an experimental value for combretastatin A-4 (**2**) from the paper in which the data were taken. Compound **2** was assigned a value of 1.0 and all others were determined by dividing the experimental IC₅₀ by the IC₅₀ of this analogue. Colchicine inhibition

Table 4. Preliminary and final non-cross-validated CoMFA values for [³H]colchicine

Compound	Preliminary non-cross-validated model (log 1/IC ₅₀)			Final non-cross-validated model (log 1/IC ₅₀)		
	obs	pred	res	obs	pred	res
2	1.99	1.99	0.006	1.99	1.99	0.0044
3	1.98	1.97	0.017	1.98	1.96	0.02
4a	1.70	1.73	−0.064	1.70	1.76	−0.06
4b	1.70	1.73	0.097			
5	1.15	1.45	−0.301	1.15	1.36	−0.21
6	1.92	1.72	0.198	1.92	1.83	0.09
7a	1.38	1.39	−0.006	1.38	1.34	0.04
7b	1.38	1.30	0.082			
8	2.00	1.99	0.005	2.00	2.02	−0.03
9a	1.89	1.80	0.092			
9b	1.89	1.98	−0.087	1.89	1.88	0.01
10a	1.86	1.91	−0.048			
10b	1.86	1.99	−0.127	1.86	1.91	−0.05
11	1.70	1.69	0.055	1.74	1.69	0.05
12	1.86	1.65	0.216	1.86	1.69	0.17
13	1.89	1.83	0.064	1.89	1.91	−0.02
14	1.78	1.86	−0.084	1.78	1.80	−0.02
15	1.49	1.53	−0.038	1.49	1.47	0.02
16a	1.79	1.72	0.070			
16b	1.79	1.78	0.016	1.79	1.89	−0.10
17a	1.40	1.38	0.021	1.40	1.37	0.03
17b	1.40	1.44	0.043			
18a	1.43	1.57	−0.134			
18b	1.43	1.49	−0.057	1.43	1.38	0.05
19a	1.91	1.94	−0.030	1.91	1.93	−0.01
19b	1.91	1.86	0.050			
20a	1.95	1.97	−0.024			
20b	1.95	1.93	0.020	1.95	1.95	0.01
21a	1.97	1.98	−0.010	1.97	2.00	−0.03
21b	1.97	2.03	−0.060			
22a	1.92	1.91	0.014	1.92	1.89	0.03
22b	1.92	1.84	0.084			

Table 5. Cross-validated PLS analysis for inhibition of tubulin polymerization

Components	Preliminary model		Final model ^a	
	s	R ²	s	R ²
1	0.465	0.009	0.508	−0.380
2	0.461	0.059	0.461	0.189
3	0.448	0.138	0.454	0.256
4	0.457	0.135	0.423	0.389
5	0.434	0.246	0.428	0.410
6	0.451	0.219	0.452	0.383

^as, standard error for the estimate of log IC₅₀; R², correlation coefficient or press value = $1.0 - \{\Sigma(Y \text{ predicted} - Y \text{ actual})^2 / \Sigma(Y \text{ actual} - Y \text{ mean})^2\}$. Optimum number of components is equal to 5. Dropped 1668 of 1800, Standard error of estimate = 0.146, R² = 0.931, *f* value (*n*₁ = 5, *n*₂ = 16) = 43.435. Prob. of R² = 0 (*n*₁ = 5, *n*₂ = 16) 0.000, relative contributions steric 0.596, electrostatic 0.404.

was used as found in the literature and all data are reported in Tables 1 and 7.

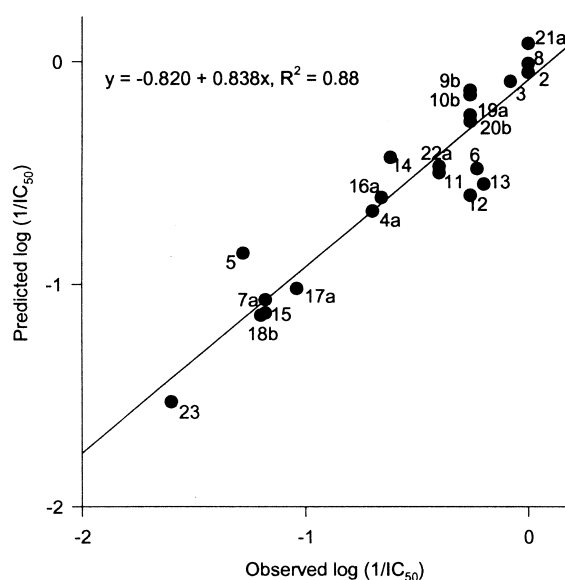
Data analysis

Statistical correlations were performed using Jandel Scientific Software. All equations and correlations were

Table 6. Cross-validated PLS analysis for % [³H]colchicine inhibition

Components	Preliminary model		Final model ^a	
	s	R ²	s	R ²
1	0.267	−0.117	0.275	−0.189
2	0.252	0.059	0.240	0.147
3	0.244	0.162	0.239	0.198
4	0.225	0.334	0.218	0.375
5	0.228	0.356	0.224	0.378
6	0.231	0.384	0.242	0.322

^as, standard error for the estimate of log IC₅₀; R², correlation coefficient or press value = $1.0 - \{\Sigma(Y \text{ predicted} - Y \text{ actual})^2 / \Sigma(Y \text{ actual} - Y \text{ mean})^2\}$. Dropped 1503 of 1600, Standard error of estimate = 0.086, R² = 0.909, *f* value (*n*₁ = 5, *n*₂ = 15) = 30.129. Prob. of R² = 0 (*n*₁ = 5, *n*₂ = 15) 0.000, relative contributions steric 0.625, electrostatic 0.375.

**Figure 3.** Plot of preliminary non-cross-validated observed versus predicted for tubulin polymerization for the training set.

calculated through the use of linear regressions based on the normalized data using SigmaStat for Windows Version 1.0. The plots shown in Figures 2–6, 9 and 10 were constructed using SigmaPlot Version 1.02a, to which the best fit linear regression line was added.

Log *P* calculations

Using experimentally determined values for the parent structures¹⁸ of biphenyl = 4.1 and benzophenone = 3.4, we estimated the log *P* values for analogues 2–30 as presented in Tables 2 and 8. To the parent structures were added the appropriate π values as follows: NHCH₃ = 0.56, NH₂ = −1.23, Cl = 0.71, Br = 0.86, F = 0.14, OH = −0.67, OCH₃ = −0.02, N(CH₃)₂ = 0.18, OAc = −0.64, C=C bond = −0.54, CH₂ or CH₃ = 0.50 and ring closure = −0.50.^{19,20} For example, the log *P* or combretastatin 13 was calculated as log *P*_{biphenyl} + 2 ($\pi_{\text{methylene}}$) + 4 (π_{methoxy}) + π_{hydroxyl} = 4.1 + 2 (0.50) + 4 (−0.02) + (−0.67) = 4.35.

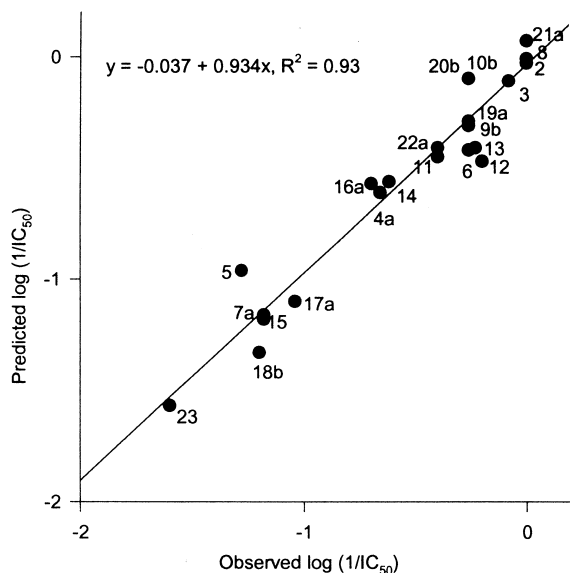


Figure 4. Plot of final non-cross-validated observed versus predicted for tubulin polymerization for the training set.

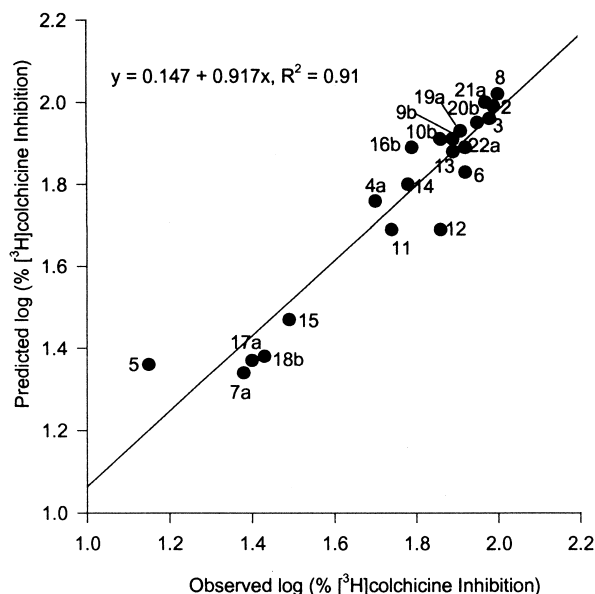


Figure 6. Plot of final non-cross-validated observed versus predicted for $[^3\text{H}]$ colchicine inhibition for the training set.

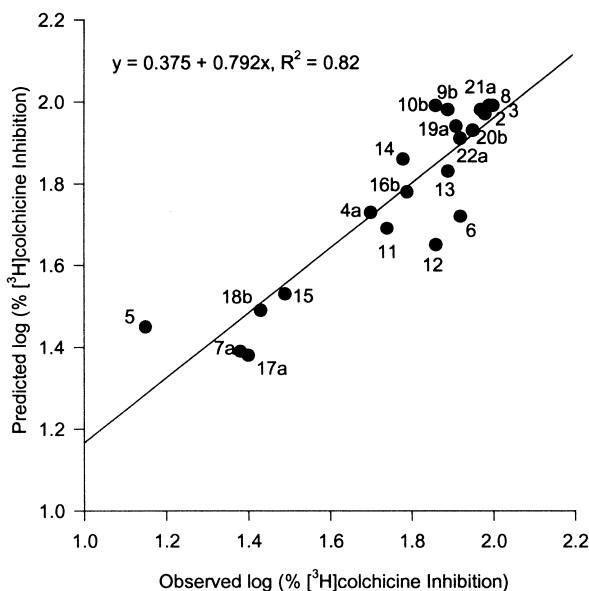


Figure 5. Plot of preliminary non-cross-validated observed versus predicted for $[^3\text{H}]$ colchicine inhibition for the training set.

Conformational analysis

We obtained X-ray structures from the Cambridge Database for colchicine (**1**),²¹ podophyllotoxin (**31**),²² and phenstatin (**32**)²³ using these as representative low energy conformations. The X-ray structure of **2** was also obtained from the Cambridge Database and used as a core to construct all unsaturated biphenyl ethylene derivatives **3–12**, **20–21** and **23–26**. In a similar fashion, 1,2-biphenyl ethane was obtained and used to construct the corresponding saturated biphenyl ethane derivatives **13–19**, **22** and **27–30**. The trimethoxy substituents on the A-ring were set, within the BUILD/EDIT mode of SYBYL, as a first approximation to the conformation

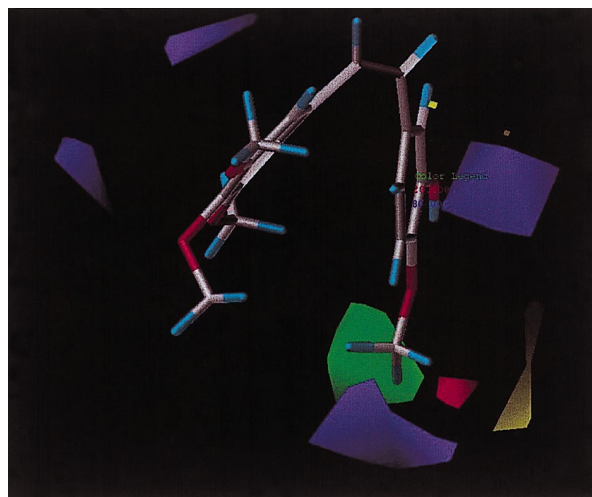


Figure 7. Steric and electrostatic CoMFA maps for inhibition of tubulin polymerization with compound **2**.

of the corresponding methoxy of the X-ray structure of colchicine. The corresponding X-ray portion of each analogue was held constant using AGGREGATE and the added functional groups were energy minimized with the Tripos force field, without solvent, using default bond angles and distances while neglecting electrostatics. In this manner, we obtained the lowest energy conformation for each compound in Tables 2 and 8. Utilizing GRIDSEARCH, we also obtained other lowest energy conformers resulting from rotation of C1, C2, C3, C4 as reported in Table 2 and chose conformation(s) that best approximated the X-ray structure of combretastatin A-4 and biphenyl ethane. We also list in Tables 2 and 8 the lowest energy conformations for all compounds containing C2 or C3 substitutions on the C-ring by searching the C2, C3, C4, C5 torsion angle as labeled in Table 1.

Charge calculations

All applied Coulson charges were calculated using AM1 (MOPAC) within SYBYL. The atomic charges were calculated in the singlet state with net charge equal to zero, keyword NOINTER and normal convergence without geometry optimization and applied to the corresponding minimized molecular structure.

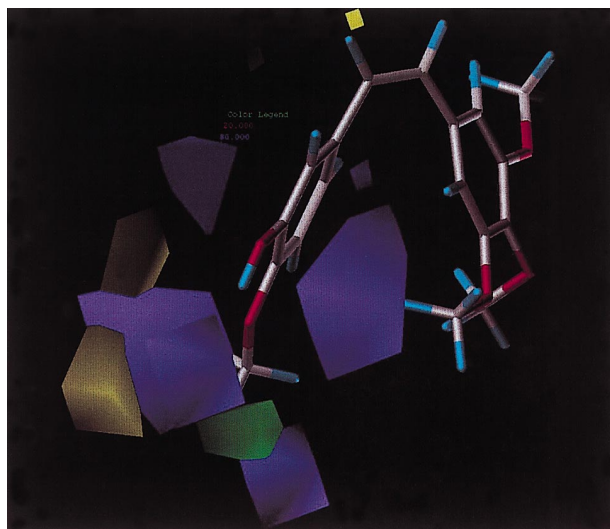


Figure 8. Steric and electrostatic CoMFA maps for inhibition of [³H]colchicine with compound **2**.

Molecular alignment

All conformations for each compound in the training set (Table 2) were aligned with the FIT routine within SYBYL without changing the low energy conformation previously obtained. All compounds were fit by aligning all six carbons of the A-ring to the corresponding carbons on the A-ring of **2**. All combretastatins in the test set (Table 8) were aligned in a similar fashion. Colchicine, phenstatin and podophyllotoxin were also aligned to **2** by overlapping the trimethoxyphenyl ring. For compounds **27–29** the stereochemistry was set to the appropriate isomer from the biological data.

CoMFA calculations

CoMFA, using default parameters except where noted, was calculated through the QSAR option of SYBYL 6.5 on a silicon graphics Octane computer. The CoMFA grid spacing was 2.0 Å in the *x*, *y*, and *z* directions, and the grid region was automatically generated by the CoMFA routine to encompass all molecules with an extension of 4.0 Å in each direction. An sp³ carbon (for sterics) and a charge of +1.0 (for electrostatics) were used as probes to generate the interaction energies at each lattice point. The default value of 30 kcal/mol was used as the maximum electrostatic and steric energy cutoff.

Partial least squares (PLS) regression analysis

Cross-validated (preliminary and final models) and non-cross-validated PLS analyses (final models for inhibition

Table 7. Observed tubulin polymerization and [³H]colchicine values for compounds composing the test set

Compd	R ₁	R ₂	R ₃	R ₄	R ₅	R ₆	R ₇	R ₈	TP inhibition	Normalized TP ^j	% [³ H] CI ^j
24	OCH ₃	OCH ₃	OCH ₃	H	H	H	OAc	OCH ₃	8.25 ^a	3.3	63 ^a
25	OCH ₃	OCH ₃	OCH ₃	H	H	OAc	OAc	OCH ₃	20 ^a	8	38 ^a
26	OCH ₃	OCH ₃	OCH ₃	H	H	H	OCH ₃	OCH ₃	4.5 ^a	1.8	56 ^a
27	OCH ₃	OCH ₃	OCH ₃	OAc (R) ^b	H	H	OH	OCH ₃	8.75 ^a	3.5	89 ^a
28	OCH ₃	OCH ₃	OCH ₃	H	OH (R) ^b	H	OH	OCH ₃	87.5 ^{a,c}	35	48 ^{a,c}
29	OCH ₃	OCH ₃	OCH ₃	OH (R) ^b	H	H	OH	OCH ₃	6.25 ^a	2.5	94 ^a
30	OCH ₃	OCH ₃	OCH ₃	H	H	H	OCH ₃	OH	ND ^d	ND ^d	12 ^a
1^e									3.2 ^h	1.7	100 ^h
31^f									2.1 ^h	1.1	88 ^h
32^g	OCH ₃	OCH ₃	OCH ₃			H	OMe	OH	1.0 ⁱ	0.83	86 ⁱ

^aReported in ref 6.

^bIndicates stereochemistry at that stereocenter.

^cReported in ref 26 as a range; 87.5 μM denotes average assigned within this range.

^dND, no data available.

^eColchicine.

^fPodophyllotoxin.

^gPhenstatin.

^hReported in ref 25.

ⁱReported in ref 4.

^jTP, tubulin polymerization; CI, colchicine inhibition.

Table 8. Physicochemical and conformational data for compounds in the test set

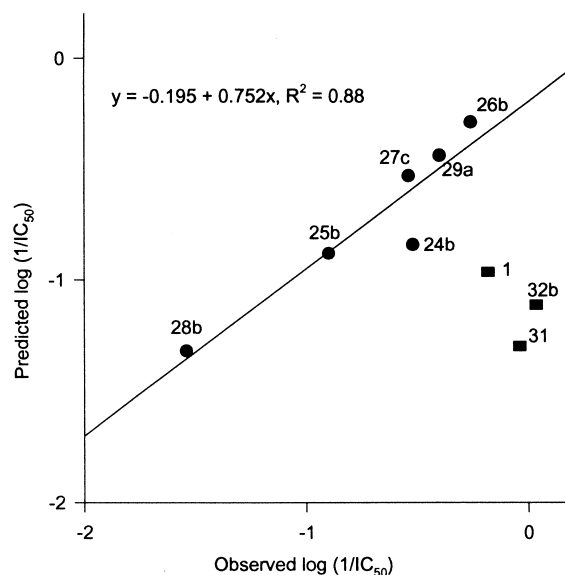
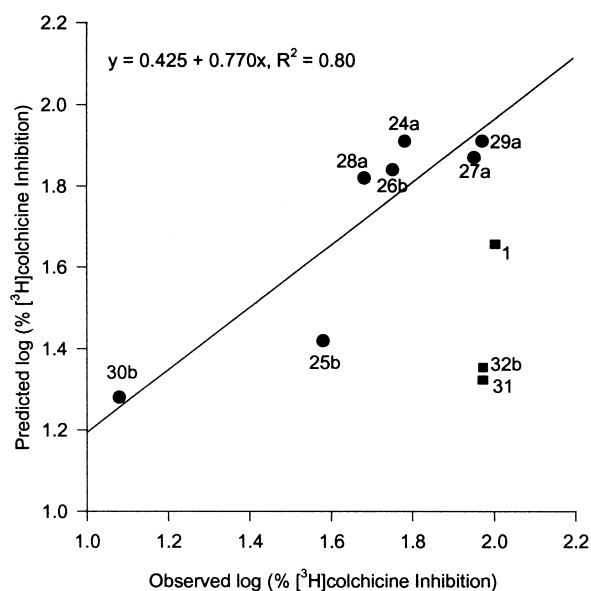
Compound	Energy (kcal/mol)	Torsion angle C1, C2, C3, C4	Torsion angle C2, C3, C4, C5	Dipole	Log <i>P</i>
24a	14.6	−3.7	135.6	3.19	2.50
24b	13.9	−3.4	−39.6	2.24	
25a	16.2	−3.7	135.0	2.49	1.86
25b	12.7	−2.8	−39.7	1.08	
26a	15.8	−3.8	136.9	2.41	3.12
26b	14.8	−3.6	−41.3	2.96	
27a	7.4	57.7	86.4	0.77	3.71
27b	6.3	56.7	86.3	2.12	
27c	13.0	57.7	−93.3	1.82	
28a	5.9	55.3	88.7	1.39	3.68
28b	5.6	45.5	−93.1	2.94	
29a	6.0	55.8	88.3	1.93	3.68
30a	7.0	50.5	85.0	2.63	4.35
30b	5.9	53.0	−96.5	2.84	
1	26.1	N.A.	N.A.	4.35	1.03 ^a
31	28.6	N.A.	N.A.	3.34	
32a	11.8	N.A.	N.A.	3.34	
32b	16.0	N.A.	N.A.	2.85	

^aReported in ref 25.**Table 9.** Predicted and actual values of inhibition of tubulin polymerization and [³H]colchicine for the test set^{a,b}

Compound	Tubulin polymerization			[³ H]Colchicine inhibition		
	pred	obs	res	pred	obs	res
24a	−0.19	−0.52		1.91	1.78	0.23
24b	−0.84	−0.52	−0.32	1.50	1.78	
25a	−0.16	−0.90		2.00	1.58	
25b	−0.88	−0.90	0.02	1.42	1.58	−0.16
26a	0.05	−0.26		2.11	1.75	
26b	−0.29	−0.26	−0.03	1.84	1.75	0.09
27a	−0.44	−0.54		1.87	1.95	−0.08
27b	−0.60	−0.54		1.81	1.95	
27c	−0.53	−0.54	0.01	1.81	1.95	
28a	−0.56	−1.54		1.82	1.68	0.14
28b	−1.32	−1.54	0.22	1.30	1.68	
29a	−0.44	−0.40	−0.04	1.91	1.97	−0.08
	−1.01	−0.40		1.52	1.97	
30a		ND		2.01	1.08	
30b		ND		1.28	1.08	0.20
1	−0.96	−0.23	0.73	1.64	2	−0.36
31	−1.33	−0.04	−1.29	1.27	1.94	−0.67
32a	−1.35	0.08		1.24	1.93	
32b	−1.17	0.08	−1.09	1.32	1.93	−0.61

^aND, no data.^bReported in ref 6 as a range 75–100; 87.5 μM denotes an arbitrary average assigned within this range.

of tubulin polymerization (Table 3) and [³H]colchicine (Table 4)) were performed within the SYBYL/QSAR routine. Separate cross-validations of the dependent columns log (1/tubulin polymerization IC₅₀) and log ([³H]colchicine inhibition) with the CoMFA columns were performed without column filtering. Analyses of the residuals reported in QSAR/REPORT QSAR were used to select a single conformation for the final model. For example, the conformer with the smallest residual **4a** was selected over **4b** in Table 3 for inclusion in the final non-cross-validated analysis. The results of the

**Figure 9.** Plot of final non-cross-validated observed versus predicted for tubulin polymerization for the test set (■ represents compounds not included in the linear regression).**Figure 10.** Plot of final non-cross-validated observed versus predicted for [³H]colchicine inhibition for the test set (■ represents compounds not included in the linear regression).

final cross-validated analyses are reported in Tables 5 and 6. As an example of our method for obtaining the non-cross-validated results, the analysis for tubulin polymerization was scaled by the CoMFA standard deviation and generated an optimum number of components equal to five and $R^2=0.41$ (Table 5). PLS analysis with non-cross-validation, performed with five components and 2 kcal/mol column filtering, resulted in dropping 1668 of 1800 columns and gave a standard error of estimate of 0.146, with a probability of $R^2=0$ ($n_1=5$, $n_2=16$) equal to 0.00, an F value ($n_1=5$, $n_2=16$) of 43.44, and a final $R^2=0.93$ (see Table 5). The relative steric (0.60) and electrostatic (0.40) contributions to the

final tubulin polymerization model were contoured as the standard deviation multiplied by the coefficient at 80% for favored steric (contoured in green) and favored positive electrostatic (contoured in blue) effects and at 20% for disfavored steric (contoured in yellow) and favored negative electrostatic (contoured in red) effects, as shown in Figure 7. In a similar manner, we derived a CoMFA model in Tables 4 and 6 using [³H]colchicine as the biological descriptor. Likewise, the final non-cross-validated analysis was also performed for correlation of log (% [³H]colchicine) and reported in Table 4 and the CoMFA electrostatic and steric maps in Figure 8. Using the appropriate CoMFA model and PREDICT PROPERTY in the QSAR module of SYBYL, we predicted inhibition of tubulin polymerization and [³H]colchicine (see Table 9) for compounds **1** and **24–32**.

Acknowledgements

Support of this work by the UNCF/Merck Science initiative on the behalf of M.L.B. is gratefully acknowledged. We also thank the University of Virginia Department of Chemistry for graduate assistance to J.M.R.

References

- Han, Y.; Malak, H.; Chaudhary, A. G.; Chordia, M. D.; Kingston, D. G.; Bane, S. *Biochemistry* **1998**, *37*, 6636.
- Pettit, G. R.; Cragg, G. M.; Herald, D. L.; Schmidt, J. M.; Lohavanijaya, P. *Can. J. Chem.* **1982**, *60*, 1374.
- Lin, C. M.; Ho, H. H.; Pettit, G. R.; Hamel, E. *Biochemistry* **1989**, *28*, 6984.
- Pettit, G. R.; Toki, B.; Herald, D. L.; Verdier-Pinard, P.; Boyd, M. R.; Hamel, E.; Pettit, R. K. *J. Med. Chem.* **1998**, *41*, 1688.
- Getahun, Z.; Jurd, L.; Chu, P. S.; Lin, C. M.; Hamel, E. *J. Med. Chem.* **1992**, *35*, 1058.
- Lin, C. M.; Singh, S. B.; Chu, P. S.; Dempcy, R. O.; Schmidt, J. M.; Pettit, G. R.; Hamel, E. *Mol. Pharm.* **1988**, *34*, 200.
- Jordan, A.; Hadfield, J. A.; Lawrence, N. J.; McGown, A. T. *Med. Res. Rev.* **1998**, *18*, 259.
- Hastie, S. B.; Macdonald, T. L. *Biochem. Pharmacol.* **1990**, *39*, 1271.
- Bane, S.; Puett, D.; Macdonald, T. L.; Williams, R. C., Jr. *J. Biol. Chem.* **1984**, *259*, 7391.
- Hastie, S. B.; Williams, R. C.; Puett, D.; Macdonald, T. L. *J. Biol. Chem.* **1989**, *264*, 6682.
- Nandy, P.; Banerjee, S.; Gao, H.; Hui, M. B.; Lien, E. J. *Pharmaceutical Res.* **1991**, *8*, 776.
- Ter Haar, E.; Rosenkranz, H. S.; Hamel, E.; Day, B. W. *Bioorg. Med. Chem.* **1996**, *4*, 1659.
- Zhu, Q.; Guo, Z.; Huang, N.; Wang, M.; Chu, F. *J. Med. Chem.* **1997**, *40*, 4319.
- Cho, S. J.; Tropsha, A.; Suffness, M.; Cheng, Y. C.; Lee, K. H. *J. Med. Chem.* **1996**, *39*, 1383.
- Quinn, F. R.; Beisler, J. A. *J. Med. Chem.* **1981**, *24*, 251.
- Quinn, F. R.; Neiman, Z.; Beisler, J. A. *J. Med. Chem.* **1981**, *24*, 636.
- Wolff, M. *Berger's Part 1: The Basis of Medicinal Chemistry*, 4th ed.; John Wiley & Sons: New York, 1980; p 298.
- Hanna, M.; de Biasi, V.; Bond, B.; Salter, C.; Hutt, A. J.; Camilleri, P. *Anal. Chem.* **1998**, *70*, 2092.
- Fujita, T.; Iwasa, J.; Hansch, C. *J. Am. Chem. Soc.* **1964**, *86*, 5175.
- Iwasa, J.; Fujita, T.; Hansch, C. *J. Am. Chem. Soc.* **1964**, *86*, 150.
- Lessinger, L.; Marguilis, T. N. *Acta Crystallogr. Sect. B* **1978**, *34*, 578.
- Anderson, K. V.; Buchardt, O.; Hansen, H. F.; Jensen, R. B.; Larsen, S. *J. Chem. Soc., Perkins Trans. 2* **1990**, 1871.
- Pettit, G. R.; Toki, B.; Herald, D. L.; Verdier-Pinard, P.; Boyd, M. R.; Hamel, E.; Pettit, R. K. *J. Med. Chem.* **1998**, *41*, 1688.
- Clark, M. D.; Cramer, R. D. III; Opdenbosch, N. V. *J. Comput. Chem.* **1989**, *10*.
- Cushman, M.; Nagarathnam, D.; Gopal, D.; Chakraborti, A. K.; Lin, C. M.; Hamel, E. *J. Med. Chem.* **1991**, *34*, 2579.
- Shi, Q.; Verdier-Pinard, P.; Brossi, A.; Hamel, E.; McPhail, A. T.; Lee, K. H. *J. Med. Chem.* **1997**, *40*, 961.